

1 Perspectives on future sea ice and navigability in the Arctic

2 Jinlei Chen¹, Shichang Kang^{1,2}, Wentao Du¹, Junming Guo¹, Min Xu¹, Yulan Zhang¹,
3 Xinyue Zhong³, Wei Zhang¹, Jizu Chen¹

4 ¹State Key Laboratory of Cryospheric Science, Northwest Institute of Eco-Environment and
5 Resources, Chinese Academy of Sciences, Lanzhou 730000, China

6 ²CAS Centre for Excellence in Tibetan Plateau Earth Sciences, Beijing 100101, China

7 ³Key Laboratory of Remote Sensing of Gansu Province, Northwest Institute of Eco-Environment
8 and Resources, Chinese Academy of Sciences, Lanzhou 730000, China

9 Correspondence: Shichang Kang (shichang.kang@lzb.ac.cn)

10 **Abstract** The retreat of sea ice has been found to be very significant in the Arctic
11 under global warming. It is projected to continue and will have great impacts on
12 navigation. Perspectives on the changes in sea ice and navigability are crucial to the
13 circulation pattern and future of the Arctic. In this investigation, the decadal changes in
14 sea ice parameters were evaluated by the multi-model from Coupled Model Inter-
15 comparison Project Phase 6, and Arctic navigability was assessed under two shared
16 socioeconomic pathways (SSPs) and two vessel classes with the Arctic transportation
17 accessibility model. The sea ice extent shows a high possibility of decreasing along
18 SSP5-8.5 under current emissions and climate change. The decadal rate of decreasing
19 sea ice will increase in March but decrease in September until 2060, when the oldest
20 ice will have completely disappeared and the sea ice will reach an irreversible tipping
21 point. Sea ice thickness is expected to decrease and transit in certain parts, declining by
22 -0.22 m per decade after September 2060. Both the sea ice concentration and volume

23 will thoroughly decline at decreasing decadal rates, with a greater decrease in volume
24 in March than in September. Open water ships will be able to cross the Northern Sea
25 Route and Norwest Passage between August and October during the period from 2045–
26 2055, with a maximum navigable area in September. The time for polar class 6 (PC6)
27 ships will shift to October–December during the period from 2021–2030, with a
28 maximum navigable area in October. In addition, the Central Passage will be open for
29 PC6 ships between September and October during 2021–2030.

30 **Keywords:** Arctic; Sea ice; Arctic Passages; Navigability; Future Changes

31 **1. Introduction**

32 The Arctic has experienced significant warming since the 1970s (Connolly et al.,
33 2017). Along with the increasing surface air temperature, Arctic communities have
34 experienced unprecedented changes, such as reduction of sea ice extent and thickness,
35 loss of the Greenland ice sheet, decrease in snow coverage, and thawing of permafrost
36 (Biskaborn et al., 2019; Box et al., 2019; Brown et al., 2017; Loomis et al., 2019). The
37 sea ice extent has declined at a rate of approximately 3.8% per decade. In comparison,
38 perennial ice had a higher proportion of loss of approximately 11.5% per decade during
39 the period from 1979–2012 (Comiso and Hall, 2014). The average ice thickness near
40 the end of the melt season decreased by 2.0 m or 66% between the pre–1990 submarine
41 period (1958–1976) and the CryoSat-2 period (2011–2018) (Kwok, 2018). Continued
42 declines in sea ice have been projected by the Coupled Model Inter-comparison Project
43 Phase 5 in the Arctic through the end of the century (Meredith et al., 2019), although
44 with some significant differences in timing (Stephenson et al., 2013).

45 Sea ice reflects a significant fraction of the solar radiation because it has a high
46 albedo. It also reduces the heat transfer between the ocean and the atmosphere as it acts
47 as an insulator (Screen and Simmonds, 2010). With the retreatment of sea ice,
48 thermohaline circulation has changed (Jourdain et al., 2017), and global warming has
49 intensified (Abe et al., 2016). However, climate change has led to prolonged open water
50 conditions and large-scale Arctic shipping that will involve ice channels (Barnhart et
51 al., 2015; Huang et al., 2020). The Northern Sea Route (NSR) extends along the
52 northern coast of Eurasia from Iceland to the Bering Strait, which shortens the transit
53 distance by approximately 15%–50% relative to the southern routes through the Suez
54 Canal (Buixadé Farré et al., 2014). It is navigable for approximately 3 months per year
55 for ice-strengthened ships at the end of summer and the beginning of autumn (Yu et al.,
56 2020). The end of shipping season for open water (OW) vessels has reached October
57 24th since 2010. However, navigability is still affected by the ice regime, such as ice
58 thickness and concentration, around the Severnaya Zemlya Islands, the Novosibirsk
59 Islands, and the East Siberian Sea (Chen et al., 2019). The Northwest Passage (NWP)
60 follows the northern coast of North America and crosses the Canadian Arctic
61 archipelago. Compared to the traditional Panama Canal route from Western Europe to
62 the Far East, the NWP shortens the transit distance by 9000 km (Howell and Yackel,
63 2004). The shortest navigable period was up to 69 days during 2006–2015 (Liu et al.,
64 2017), and the first time being completely free of ice was reported to occur in September
65 2007 (Cressey, 2007). Geographical and political factors also pose some challenges to
66 the navigability of passages and choice of routes (Ryan et al., 2020). The straits along

67 the NWP are at times narrow and shallow, which are easily clogged by free floating ice.
68 NSR is greater than NWP in terms of geography, while it still has several choke points
69 where ships must pass through shallow straits between islands and the Russian
70 mainland (Streng et al., 2013). Apart from the geographical factor, the various
71 organizations and groups formed between the surround-Arctic nations, as well as the
72 disputes and agreements, give impetuses for adopting the NSR. Russia has committed
73 several large infrastructure projects to support the NSR, such as Yamal-Nenets railway
74 and emergency rescue centers (Serova, N. A. and Serova, V. A, 2019). China, which is
75 characterized as a near-Arctic state, also outlined the plans to build a Polar Silk Road
76 by building infrastructure and conducting trial voyages (Tillman et al., 2019). For the
77 development of socioeconomics and marine transportation, future projections to ice
78 conditions and Arctic Passages are increasingly important, in which climatic changes
79 should be considered (Gascard et al., 2017). Smith and Stephenson (2013) investigated
80 the potential of Arctic Passages under representative concentration pathways (RCP) 4.5
81 and RCP 8.5 and found that OW ships and Polar Class 6 (PC6) ships (Table 1) were
82 able to cross NSR and NWP in September in the mid-century, respectively. The areas
83 of the Arctic accessible to PC3, PC6, and OW ships would rise to 95%, 78%, and 49%,
84 respectively, of the circumpolar International marine Organization Guidelines
85 Boundary area by the late 21st century (Stephenson et al., 2013). Melia et al. (2017)
86 suggested that the Arctic Passages from Europe to Asia would be 10 days faster than
87 conventional routes by the mid-century and 13 days faster by the late century. Recent
88 research has shown that NSR might be accessible earlier for OW ships in September

89 2021–2025, and the navigable window would extend to August–October during 2026–
90 2050 under shared socioeconomic pathways (SSPs) 2–4.5 (Chen et al., 2020). However,
91 evaluating sea ice conditions and Arctic navigability by a single climate model, even
92 one with a higher resolution, is insufficient.

93 This prospective study was designed to obtain further insight into the future
94 changes in sea ice in the Arctic and the navigability of the Arctic during this century
95 with ensemble-up-to-date climate models in the Coupled Model Inter-comparison
96 Project Phase 6 (CMIP6). To reduce uncertainties of a single high resolution model and
97 multi-model average, models were filtered by comparing the historical simulations and
98 observations of sea ice extent, and the possible SSPs were investigated with the average
99 of multiple models. The distributions of the linear trend of sea ice extent, concentration,
100 and thickness were explored in three stages (2021–2040, 2041–2060, and 2061–2100).
101 In addition, the changes in sea ice volume and age were analyzed. The accessibility of
102 the Arctic and the navigable area were evaluated with the Arctic Transportation
103 Accessibility Model (ATAM) from the Arctic Ice Regime Shipping System (AIRSS)
104 for OW ships and PC6 ships under SSP2–45 and SSP5–85 in 2021–2030 and 2045–
105 2055, respectively.

106 **2. Methods**

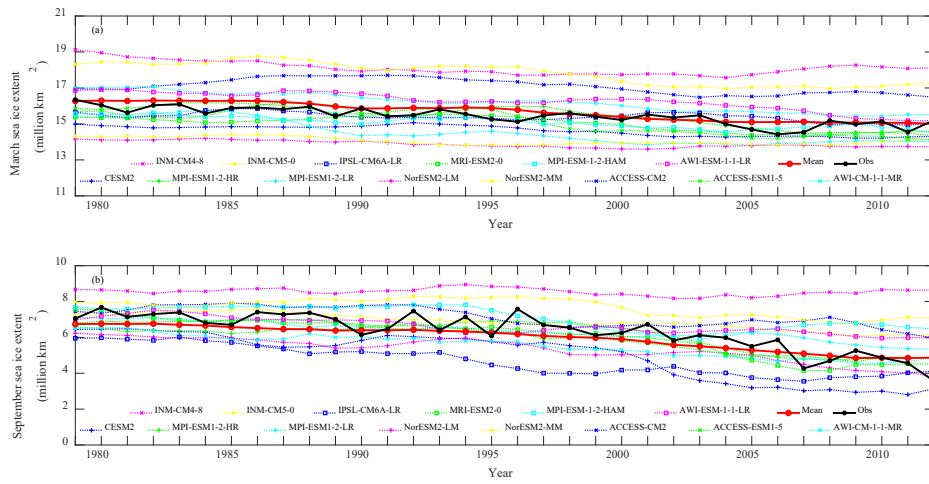
107 **2.1. Data and Model Selection**

108 The new scenario framework–SSP in CMIP6 was designed to carry out research
109 on climate change impacts and adaption by combining pathways of future radiative
110 forcing and climate changes with socioeconomic development (O’Neill et al., 2014).

111 SSP1 indicates a sustainable development, which proceeds at a reasonably high pace.
112 Technological change is rapid, inequalities are lessened and directed toward
113 environmentally friendly processes. Unmitigated emissions are high in SSP3. It is due
114 to a rapidly growing population, moderate economic growth, and slow technological
115 change in the energy sector. SSP2 is an intermediate case between SSP1 and SSP3.
116 SSP5 occurs in the absence of climate policies, energy demand is high and most of this
117 demand is met with carbon-based fuels.

118 Compared with CMIP5 models, the CMIP6 multi-model ensemble mean provides
119 a more realistic estimate of the Arctic sea ice extent (SIMIP Community, 2020), but the
120 biases of the models are still large (Shu et al., 2020). This study selected models by
121 comparing the historical trend of Arctic sea ice extent in simulation with remote sensing
122 observation during 1979–2012. The observation data comes from Sea Ice Index in the
123 National Snow & Ice Data Center. The selected models are those the correlation
124 coefficient between original simulation and observation greater than 0.8 (0.7 for March).
125 Five-point moving averages of simulations were made in Figure 1. The models passing
126 the test are CESM2, MPI-ESM1-2-HR, MPI-ESM1-2-LR, NorESM2-LM, NorESM2-
127 MM, ACCESS-ESM1-5, AWI-CM-1-1-MR, and AWI-ESM-1-1-LR in September and
128 CESM2, MPI-ESM1-2-LR, ACCESS-ESM1-5, AWI-CM-1-1-MR, INM-CM5-0,
129 MPI-ESM-1-2-HAM, and AWI-ESM-1-1-LR in March. The mean of the selected
130 models corresponds well with the observations, and the correlation coefficients are
131 0.884 and 0.817 in September and March, respectively. However, sea ice datasets in
132 SSP1-2.6, SSP2-4.5, SSP3-7.0, and SSP5-8.5 after 2020 have not been released on

133 CESM2, MPI-ESM-1-2-HAM, and AWI-ESM-1-1-LR until now. In addition, AWI-
 134 CM-1-1-MR was excluded from analyzing the navigability of the Arctic in the absence
 135 of sea ice concentration. The spatial resolution of monthly sea ice concentration and
 136 thickness was normalized to $1^\circ \times 1^\circ$ by bilinear interpolation. Variables in figures and
 137 tables were from the ensemble means of selected models.



138
 139 **Figure 1.** The observations and five-point moving averages of sea ice extent in March and
 140 September during 1979–2012.

141 2.2. Accessibility Evaluation

142 Safety and pollution are two of the opposite factors considered in developing
 143 regulatory transport standards. AIRSS was designed to minimize the risk of pollution
 144 in the Arctic due to damage to vessels by ice (Transport Canada, 1998). ATAM,
 145 developed by AIRSS, is commonly used to quantify the temporal and spatial
 146 accessibilities in the Arctic, in which the ice number (IN) represents the ability of a ship
 147 to enter ice-covered water:

$$148 \quad IN = (C_a * IM_a) + (C_b * IM_b) + \dots + (C_n * IM_n) \quad (1)$$

149 where C_a , C_b , and C_n are the sea ice concentrations. IM_a , IM_b , and IM_n are

150 the ice multipliers. a , b , and n , are ice within a range of thicknesses corresponding to
 151 IMs in equation (2). They indicate the severity of each ice type for the vessel and range
 152 from -4 to 2. Positive IM and IN represent less risk to the vessel and safe region for
 153 navigation, respectively. Vessel class reflects the structural strength, displacement, and
 154 power of a ship to break ice. PC6 ships and OW ships are vessels with moderate ice
 155 strengthening and without ice strengthening, respectively (IMO, 2002). In this paper,
 156 the navigability of the Arctic for these two kinds of ships was investigated under SSP2-
 157 45 and SSP5-85. The corresponding IMs for the OW and PC6 ships are as follows:

$$\begin{aligned}
 IM_{OW} = & 2, \text{ if } SIT = 0 \text{ cm,} \\
 & 1, \text{ if } 0 \text{ cm} < SIT < 15 \text{ cm,} \\
 & -1, \text{ if } 15 \text{ cm} \leq SIT < 70 \text{ cm,} \\
 & -2, \text{ if } 70 \text{ cm} \leq SIT < 120 \text{ cm,} \\
 & -3, \text{ if } 120 \text{ cm} \leq SIT < 151 \text{ cm,} \\
 & -4, \text{ if } SIT \geq 151 \text{ cm}
 \end{aligned} \tag{2}$$

$$\begin{aligned}
 IM_{PC6} = & 2, \text{ if } 0 \text{ cm} \leq SIT < 70 \text{ cm,} \\
 & 1, \text{ if } 70 \text{ cm} \leq SIT < 120 \text{ cm,} \\
 & -1, \text{ if } 120 \text{ cm} \leq SIT < 151 \text{ cm,} \\
 & -3, \text{ if } 151 \text{ cm} \leq SIT < 189 \text{ cm,} \\
 & -4, \text{ if } SIT \geq 189 \text{ cm}
 \end{aligned} \tag{3}$$

160
 161
 162
 163

Table 1 Vessel classes versus operating ice thickness

Vessel class	Maximum allowable ice type	Ice thickness (cm)
Polar class 3	Second year	No limit
Polar class 6	Medium first-year	0–120
Ordinary merchant	Open water/Grey	0–15

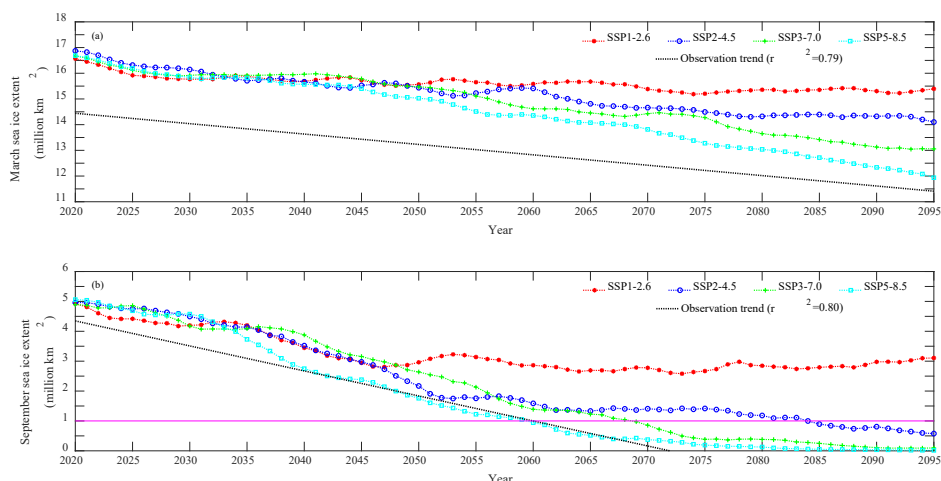
164
 165

166 **3. Results**

167 **3.1. Future Changes in Sea Ice Area and Extent**

168 The extent and area are the most reliable products of sea ice from satellite retrieval
169 (Comiso, 2012 Notz, 2014). Therefore, the remaining sea ice was taken as an indicator
170 to evaluate models and future scenarios. As shown in Figure 2, the observation trends
171 were made with least square regression of historical ensemble averages from 1979 to
172 2019, in which sea ice might completely disappear in September after 2073. In addition
173 to the classical pathways, such as SSP1-2.6, SSP2-4.5, and SSP5-8.5, CMIP6 provides
174 a variety of new selections. However, SSP1-1.9, SSP4-3.4, and SSP4-6.0 were not
175 discussed in the multi-scenario evaluation for the less released models. According to
176 historical development and scenarios, sea ice will retreat in the future with a more
177 significant decreasing trend in September. The difference between SSPs and
178 observation trends is greater in March than in September, while both have large
179 dispersions among pathways after 2050. Compared with others, SSP5-8.5 has the
180 greatest correlation coefficients, which are 0.784 and 0.712 in September and March,
181 respectively, with the observation trend; SSP2-4.5 comes second. This suggests that
182 Arctic sea ice might be the worst scenario in the future under the current emission and
183 climate change trends. The Arctic is regarded as “ice free” when the sea ice area is less
184 than 1 million km² (Lenton et al., 2019). This will occur in September 2060 with high
185 probability, and ice will almost completely disappear under SSP2-4.5, SSP3-7.0, and
186 SSP5-8.5 by the end of the century.

187



188

189 **Figure 2.** Sea ice extent under multiple scenarios and observation trends in March and September

190 “Ice free” was taken as one of the tipping points of climate change with

191 significant irreversible effects (Lenton et al., 2019). Three stages were extracted for the

192 changes in sea ice extent in Figure 3. Decadal linear trends and probability distributions

193 with an interval of 0.4 were calculated to evaluate the decline in sea ice and the

194 difference in models. Sea ice linear trends are less than zero in both March and

195 September in 2021–2100, while the retreat will be more remarkable in September

196 before 2060, especially during 2021–2040, after which the decline is mainly shown in

197 March because the extent might be close to “ice free” in September. The dispersion of

198 SSPs will increase in March over time, as will the absolute decadal trends of SSP3-7.0

199 and SSP5-8.5. However, it is aggregated in September, and the decadal variability in

200 SSPs, especially SSP2-4.5 and SSP5-8.5, has a decreasing trend. Multi-model

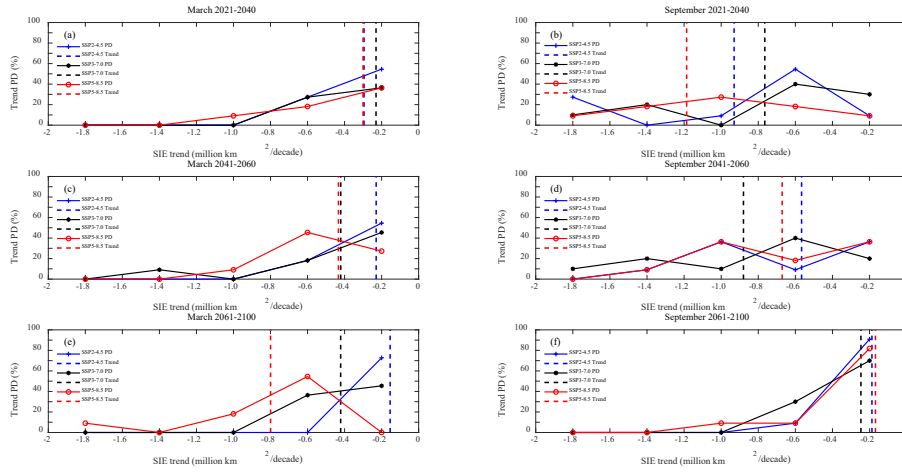
201 simulations mainly range from -0.8 to 0 million km² per decade in March, in which the

202 distributions of SSP5-8.5 are chiefly [-0.4, 0), [-0.8, -0.4), and [-0.8, -0.4) million km²

203 per decade during 2021–2040, 2041–2060, and 2061–2100, respectively. A relatively

204 even distribution is shown in September before the mid-century, while it is concentrated

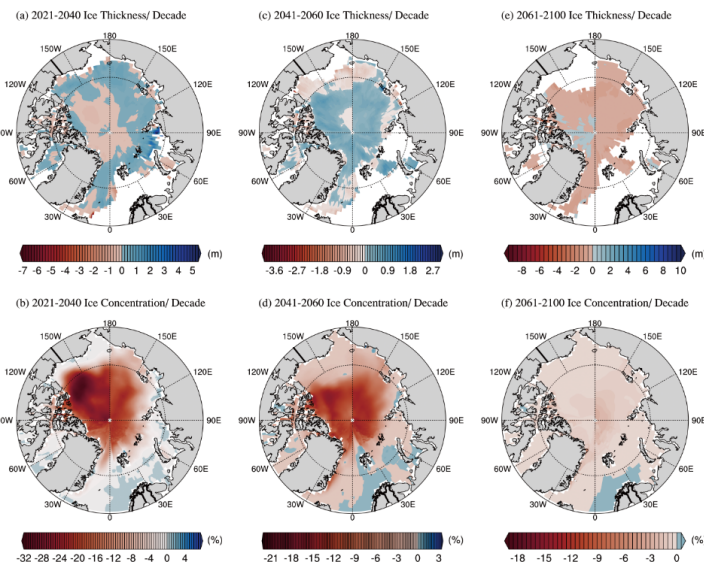
205 in $[-0.4, 0)$ in the late century. This indicates that the difference among models is still
 206 great in September before 2060, while the results are reliable in 2061–2100.



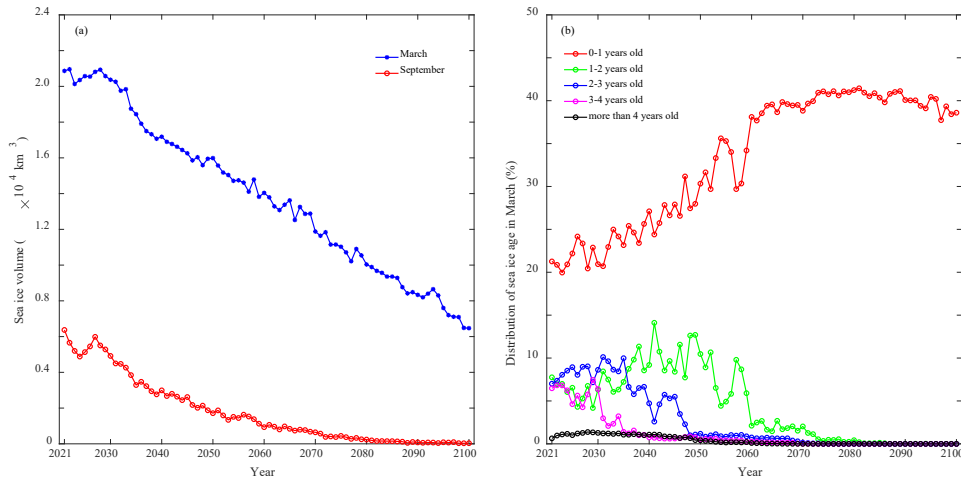
207
 208 **Figure 3.** Linear trends and probability distributions (PD) of Arctic sea ice extent (SIE) in
 209 March and September

210 **3.2. Future Changes in Other Sea Ice Parameters**

211



212
 213 **Figure 4.** Linear trends of sea ice thickness and concentration under SSP5-85 in September



214

215

Figure 5. The changes in sea ice volume and age under SSP5-85

216

217

218

219

220

221

222

223

224

225

226

227

228

229

230

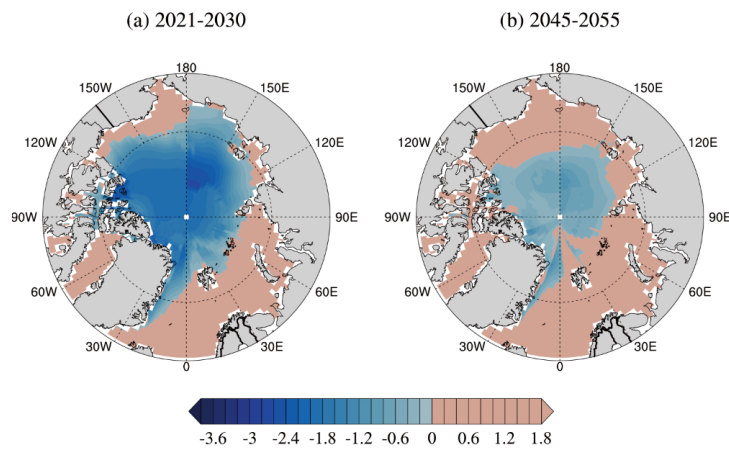
In addition to the extent and area, thickness, concentration, volume, and age are important indicators of changes in sea ice in the future. Figures 4 and 5 show the linear trends of ice thickness and concentration and the changes in sea ice volume and age, respectively, under SSP5-85 in 2021–2100. Ice thickness has a negative trend within the Arctic Archipelago, in coastal water, and in the sector to the north of the Arctic Archipelago and Greenland in September, while the other parts will slightly increase in the next 20 years. The trend is reversed in the Arctic Ocean, and the decreasing area near the shore will extend to the north in 2041–2060, after which almost all sea ice will be reduced with an average trend of -0.22 m per decade in the Arctic. Sea ice concentration will decrease throughout the rest of this century. The significant area is to the north of the Arctic Archipelago and Greenland and the Arctic Basin in September 2021–2040. The extent will shrink, and the decadal linear rate will decrease until the second half of the century, when the rate of decrease will be even and small in the Arctic. The average decadal rates of sea ice concentration are -12.39% , -6.26% , and -0.81% in the three stages. Sea ice volume will decrease in both March and September 2021–

231 2100. The rate of decrease is higher in March, and sea ice might completely disappear
232 in September before 2090. Ice age is also a key descriptor of the state of sea ice cover.
233 Compared to younger ice, older ice tends to be thicker and more resilient to changes in
234 atmospheric and oceanic forcing (Richter-Menge et al., 2019). The oldest ice (>4 years
235 old) currently comprises just a small fraction in March, and it might eventually
236 disappear at approximately the mid-century. With the degeneration of older ice, the
237 extent of the younger ice will increase over a period, such as 3- to 4-year-old ice in the
238 next 10 years, 2- to 3-year-old ice before 2035, and 1- to 2-year-old ice before 2050,
239 after which it will degrade into next younger ice. First-year ice dominates the sea ice
240 cover in the present and future. It increases mainly before 2060 and remains stable until
241 2090, after which it starts to decrease due to the lack of supplementation from degraded
242 older ice.

243 **3.3. Future Changes in Arctic Navigability**

244 With the retreatment of sea ice, the possibility for navigation is rising in the Arctic.
245 The opening of passages will be profitable for ocean shipping companies (Chang et al.,
246 2015). The most likely navigable window is in September. Figure 6 shows Arctic
247 accessibility for the OW ships under SSP5-8.5 in September. The probability of
248 crossing NSR and NWP is low in the next 10 years. The impassable areas for NSR are
249 mainly in the East Siberian Sea and northwestern Laptev Sea, but nearshore waters
250 might be navigable for vessels with shallow drafts. Four crucial straits, the Vilkitsky
251 Strait, Shokalskiy Strait, Dmitrii Laptev Strait, and Sannikov Strait, are accessible for
252 OW ships. NWP is impassable in the sectors west of Banks Island and Queen Elizabeth

253 Island, as well as the M'Clure Strait, Viscount-Melville Sound, Barrow Strait, and
 254 Lancaster Strait within the Parry Channel. All routes provided in the Arctic marine
 255 shipping assessment report (AMSA, 2009) are under restrictions for OW ships. In the
 256 mid-century, both NSR and NWP will open for OW ships under SSP5-8.5 in September.

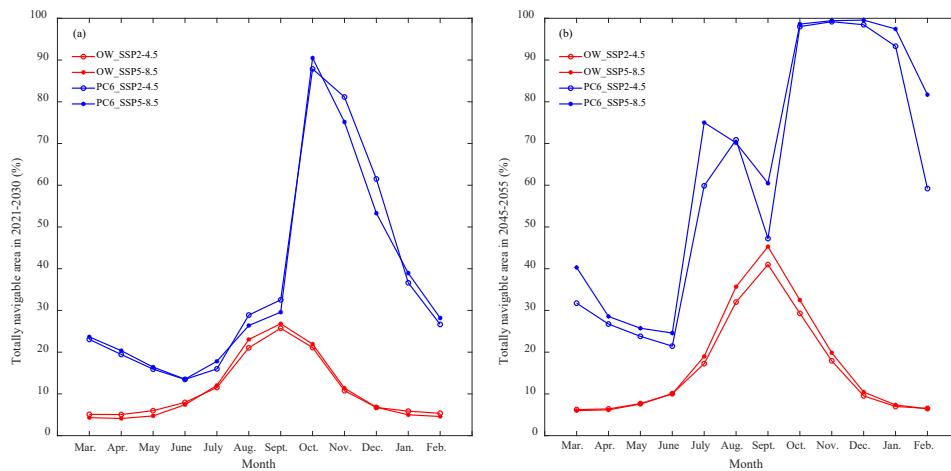


257
 258

Figure. 6. INs for OW ships under SSP5-8.5 in September

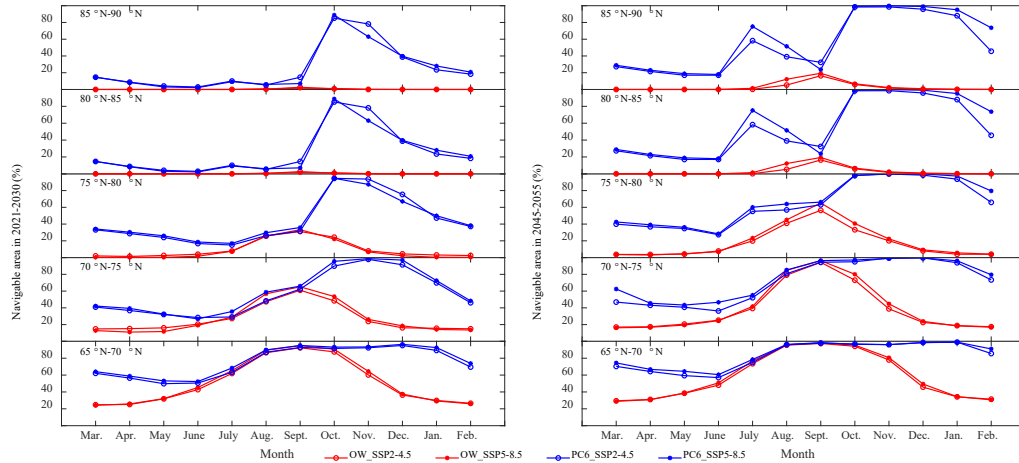
259 The opening of the Arctic Passages mainly depends on the connectivity among
 260 grids, during which the potential of individual units, which might connect with other
 261 units in the next period, is usually ignored. The overall navigable potential in a region
 262 can be measured by the percentage of accessible grids with total grids. Figure 7 displays
 263 the Arctic navigable area for OW ships and PC6 ships under SSP2-4.5 and SSP5-8.5 in
 264 2021–2030 and 2045–2055. It is the percentage of grids where INs are greater 0. The
 265 totally navigable area for OW ships is shown as a unimodal curve in both stages, with
 266 the peak in September and the valley in April and March. It is an irregular curve for
 267 PC6 ships with the minimum value in June. The maximum values are shown in October
 268 2021–2030, while they range in November and December in the mid-century. Actually,
 269 the Arctic would be navigable for PC6 ships from October to December. It is very
 270 strange that an abnormal decrease occurs in September in 2045–2055. The navigable

271 area within every 5 latitude degrees from 65°N to 90°N is plotted in Figure 8 for further
 272 study. This indicates that the abnormal point results from the decrease within 85°N–
 273 90°N, but the reason is hard to explain. The navigable area is mainly concentrated at
 274 65°N–75°N for OW ships in the next 10 years, and it will extend to 80°N in the mid-
 275 century. The central passage might be accessible for PC6 ships in September and
 276 October, and the open window would be from October to January in 2045–2055. The
 277 routes of NSR and NWP are mainly distributed in 70°N–75°N. The possibility for OW
 278 ships crossing two passages is low until August–October 2045–2055, while it is high
 279 for PC6 ships during October–December 2021–2030, and the open window would
 280 extend to August–January in 2045–2055.



281

282 **Figure 7.** Totally navigable areas for OW ships and PC6 ships under SSP2-4.5 and SSP5-8.5



283

284 **Figure 8.** Navigable areas for OW ships and PC6 ships under SSP2-4.5 and SSP5-8.5 within
 285 different latitudes

286 **4. Discussion and concluding remarks**

287 The Arctic warming rate is more than double the global average, and it has had
 288 great impacts on the Arctic and globe (Cohen et al., 2020). This paper investigated the
 289 future changes in sea ice and navigability of passages in the Arctic under two kinds of
 290 shared socioeconomic pathways. It provides a vision of the earth's future and has great
 291 significance for navigation planning. The following results were found.

- 292 (1) The changes in sea ice would occur along SSP5-8.5 with a higher possibility under
 293 the current trend. "Ice free" might appear in September 2060, and sea ice would
 294 completely disappear by the end of the century.
- 295 (2) The retreat of sea ice is more significant in September before 2060, after which the
 296 decline is mainly shown in March. The decadal sea ice extent will increase under
 297 SSP5-8.5 in March but decrease in September.
- 298 (3) The decrease in sea ice thickness will transit from the Arctic Ocean north of the
 299 Arctic Archipelago and Greenland to the seas along Russia and North America
 300 and will totally decline with an average decadal trend of -0.22 m in September

301 after 2060. Sea ice concentration will thoroughly decline with decreasing decadal
302 rates.

303 (4) Sea ice volume will decrease at a higher decadal rate in March than in September.

304 The oldest ice might eventually disappear at approximately the mid-century. First
305 year ice dominates the sea ice cover. It increases mainly before 2060 and remains
306 stable until 2090, after which it starts to decrease.

307 (5) The probability for OW ships crossing NSR and NWP is low in 2021–2030, while
308 it is high in August–October 2045–2055, with maximum and minimum navigable
309 areas in September and March, respectively.

310 (6) The passages along the coast and crossing the Arctic might open for PC6 ships
311 during October–December and September–October 2021–2030, respectively, with
312 a maximum navigable area in October. The open window would extend to August–
313 January and October–January in 2045–2055, respectively, and the maximum
314 navigable area ranges in November and December.

315 The navigable window for OW ships and PC6 ships along the NSR were
316 investigated in our previous work (Chen et al., 2020), but it is deficient to evaluate
317 Arctic navigability by a single climate model, even with a high resolution. This study
318 serves as a reference for future changes in sea ice and navigability in the Arctic,
319 including NSR, NWP, and Central Passage. However, the uncertainty of the models
320 might have affected the results and their reliability in this research. Approximated
321 physical processes and unreal parameters in models are inevitable problems in the
322 geosciences. Differences still existed even when the models were filtered by comparing

323 the historical simulations with the observations of sea ice extent. The abnormal decrease
324 in navigable area at high latitudes (80°N–90°N) in September might be an example.
325 This is against conventional wisdom, but it could be true. The uncertainty of the models
326 is expected to decrease in future prospective research. Different ice types do make a big
327 difference to ship navigability. For example, for the same ice thickness * ice
328 concentration (e.g. SIT * SIC = 0.3), pack ice (say SIT = 0.6 m thick and SIC = 50%)
329 have a high degree of freedom that level ice (say SIT = 0.3 m and SIC = 100%) doesn't
330 have. Thus, ships are easier to navigate in broken ice floes (Huang et al., 2020). ATAM
331 is hard to clearly distinguish ice types at first, and this might be a future direction.

332

333 *Data Availability.* All the data used in this paper are available online. The simulations
334 to sea ice can get from the CMIP6 (<https://esgf-node.llnl.gov/search/cmip6/>). The
335 observation of sea ice extent is available from the National Snow & Ice Data Center
336 (<https://nsidc.org/data/G02135/versions/3>).

337

338 *Author contributions.* JLC and SK developed the concept, and investigated the methods
339 of this paper. JLC and WD analyzed the data and wrote the original draft. JG, MX, XZ,
340 WZ and JZC reviewed and edited the manuscript.

341

342 *Competing interests.* The authors declare that they have no conflict of interest.

343

344 *Acknowledgements* Thanks for the data from CMIP6 and NSIDC. Our cordial gratitude

345 should be extended to anonymous reviewers and the Editors for their professional and
346 pertinent comments on this manuscript.

347

348 **Financial support.** This work was financially supported by the National Natural
349 Science Foundation of China (41721091), the Frontier Science Key Project of CAS
350 (QYZDY-SSW-DQC021, and QYZDJ-SSW-DQC039), , the State Key Laboratory of
351 Cryospheric Science (SKLCS-ZZ-2021), the China National Key Research and
352 Development Program (2020YFA0608500, and 2020YFA0608503), and Foundation
353 for Excellent Youth Scholars of “Northwest Institute of Eco-Environment and
354 Resources”, CAS (FEYS2019020).

355

356 **References**

357 Abe, M., Nozawa, T., Ogura, T., & Takata, K.: Effect of retreating sea ice on
358 Arctic cloud cover in simulated recent global warming, *Atmos. Chem. Phy*
359 *s.*, 16, 14343–14356, <https://doi.org/10.5194/acp-16-14343-2016>, 2016.

360 AMSA: Arctic marine shipping assessment 2009 report. Arctic Council, 2009.

361 Barnhart, K. R., Miller, C. R., Overeem, I., and Kay, J. E.: Mapping the future
362 expansion of Arctic open water, *Nat. Clim. Change*, 6, 280–285, [https://doi.o](https://doi.org/10.1038/nclimate2848)
363 [rg/10.1038/nclimate2848](https://doi.org/10.1038/nclimate2848), 2015.

364 Biskaborn, B. K., Smith, S. L., Noetzli, J., Matthes, H., Vieira, G., Streletskiy,
365 D. A.: Permafrost is warming at a global scale, *Nat. Commun.*, 10, [https://](https://doi.org/10.1038/s41467-018-08240-4)
366 doi.org/10.1038/s41467-018-08240-4, 2019.

367 Box, J. E., Colgan, W. T., Christensen, T. R., Schmidt, N. M., Lund, M., Par
368 mentier, F.-J. W.: Key indicators of Arctic climate change: 1971–2017, *En*
369 *viron. Res. Lett.*, 14, 045010, <https://doi.org/10.1088/1748-9326/aafc1b>, 201

370 9.

371 Brown, R., Vikhamar Schuler, D., Bulygina, O., Derksen, C., Luojus, K., Mudr
372 yk, L.: Arctic terrestrial snow cover. *Snow, Water, Ice and Permafrost in*
373 *the Arctic (SWIPA) 2017*, Arctic Monitoring and Assessment Programme
374 (AMAP), Oslo, Norway, 25–64, 2017.

375 Buixadé Farré, A., Stephenson, S. R., Chen, L., Czub, M., Dai, Y., Demchev,
376 D.: Commercial Arctic shipping through the Northeast Passage: routes, reso
377 urces, governance, technology, and infrastructure, *Polar Geography*, 37, 298
378 –324. <https://doi.org/10.1080/1088937x.2014.965769>, 2014.

379 Chang, K. Y., He, S. S., Chou, C. C., Kao, S. L., Chiou, A. S.: Route planni
380 ng and cost analysis for travelling through the Arctic Northeast Passage us
381 ing public 3D GIS. *Int. J. Geogr. Inf. Sci.*, 29, 7–8, 1375–1393, [https://do](https://doi.org/10.1080/13658816.2015.1030672)
382 [i.org/10.1080/13658816.2015.1030672](https://doi.org/10.1080/13658816.2015.1030672), 2015.

383 Chen, J. L., Kang, S. C., Chen, C. S., You, Q. L., Du, W. T., Xu, M.: Chang
384 es in sea ice and future accessibility along the Arctic Northeast Passage,
385 *Global Planet. Change*, 195, 103319, [https://doi.org/10.1016/j.gloplacha.2020.](https://doi.org/10.1016/j.gloplacha.2020.103319)
386 [103319](https://doi.org/10.1016/j.gloplacha.2020.103319), 2020.

387 Chen, S. Y., Cao, Y. F., Hui, F. M., and Cheng, X.: Observed spatial-temporal
388 changes in the autumn navigability of the Arctic Northeast Route from 2
389 010 to 2017 (in Chinese), *Chinese Sci. Bull.*, 64, 1515–1525, [https://doi.or](https://doi.org/10.1360/N972018-01083)
390 [g/10.1360/N972018-01083](https://doi.org/10.1360/N972018-01083), 2019.

391 Cohen, J., Zhang, X., Francis, J. A., Jung, T., Kwok, R., Overland, J.: Diverge
392 nt consensus on Arctic amplification influence on midlatitude severe wint
393 er weather, *Nat. Clim. Change*, 10, 20–29, [http://doi.org/10.1038/s41558-01](http://doi.org/10.1038/s41558-019-0662-y)
394 [9-0662-y](http://doi.org/10.1038/s41558-019-0662-y), 2020.

395 Comiso, J. C.: Large decadal decline of the Arctic multiyear ice cover, *J. Cli*
396 *mate*, 25, 1176–1193, <https://doi.org/10.1175/JCLI-D-11-00113.1>, 2012.

397 Comiso, J. C., and Hall, D. K.: Climate trends in the Arctic as observed from

398 space, *Wires. Clim. Change*, 5, 389–409, <https://doi.org/10.1002/wcc.277>, 20
399 14.

400 Cressey, D.: Arctic melt opens Northwest Passage, *Nature*, 449, 267–267. <https://doi.org/10.1038/449267b>, 2007.

401

402 Gascard, J.-C., Riemann-Campe, K., Gerdes, R., Schyberg, H., Randriamampiani
403 na, R., Karcher, M.: Future sea ice conditions and weather forecasts in the
404 Arctic: Implications for Arctic shipping, *Ambio*, 46, 355–367, [https://doi.or
405 g/10.1007/s13280-017-0951-5](https://doi.org/10.1007/s13280-017-0951-5), 2017.

406 Howell, S. E. L., and Yackel, J. J.: A vessel transit assessment of sea ice vari
407 ability in the Western Arctic, 1969–2002: implications for ship navigation,
408 *Can. J. Remote Sens.*, 30, 205–215, <https://doi.org/10.5589/m03-062>, 2004.

409 Huang, L. F., Li, M. H., Romu, T., Dolatshah, A., Thomas, G.: Simulation of
410 a ship operating in an open-water ice channel. *Ships Offshore Struc.*, <https://doi.org/10.1080/17445302.2020.1729595>, 2020.

411

412 Huang, L. F., Tuhkuri, J., Igreg, B., et al.: Ship resistance when operating in f
413 loating ice floes: a combined CFD&DEM approach. *Mar. Struct.*, 74, 1028
414 17, <https://doi.org/10.1016/j.marstruc.2020.102817>, 2020.

415 IMO: Guidelines for ships operating in Arctic ice-covered waters, In: MSC/Circ.1056
416 and MEPC/Circ.399, 2002.

417 Jourdain, N. C., Mathiot, P., Merino, N., Durand, G., Le Sommer, J., Spence,
418 P.: Ocean circulation and sea-ice thinning induced by melting ice shelves i
419 n the Amundsen Sea, *J. Geophys. Res-Oceans*, 122, 2550–2573, [https://doi.
420 org/10.1002/2016jc012509](https://doi.org/10.1002/2016jc012509), 2017.

421 Kwok, R.: Arctic sea ice thickness, volume, and multiyear ice coverage: losses
422 and coupled variability (1958–2018), *Environ. Res. Lett.*, 13, 105005, <https://doi.org/10.1088/1748-9326/aae3ec>, 2018.

423

424 Lenton, T., Rockström, J., Gaffney, O., Rahmstorf, S., Richardson, K., Steffen,
425 W.: Climate tipping points-too risky to bet against, *Nature*, 575, 592–595,
426 <https://doi.org/10.1038/d41586-019-03595-0>, 2019.

427 Liu, X., Ma, L., Wang, J., Wang, Y., and Wang, L.: Navigable windows of th

428 e Northwest Passage, *Polar Sci.*, 13, 91–99, <https://doi.org/10.1016/j.polar.20>
429 17.02.001, 2017.

430 Loomis, B. D., Rachlin, K. E., and Luthcke, S. B. Improved Earth oblateness r
431 ate reveals increased ice sheet losses and mass - driven sea level rise. *Geo*
432 *phys. Res. Lett.*, 46, 6910–6917, <https://doi.org/10.1029/2019gl082929>, 201
433 9.

434 Melia, N., Haines, K., Hawkins, E., and Day, J. J.: Towards seasonal Arctic sh
435 ipping route predictions. *Environ. Res. Lett.*, 12, 084005, <https://doi.org/10.1>
436 088/1748-9326/aa7a60, 2017.

437 Meredith, M. P., Sommerkorn, M., Cassotta, S., Derksen, C., Ekaykin, A. A.,
438 Hollowed, A.: Chapter 3: Polar Regions. IPCC special report on the ocean
439 and cryosphere in a changing climate, In press. <https://report.ipcc.ch/srocc/>
440 [pdf/SROCC_FinalDraft_FullReport.pdf](https://report.ipcc.ch/srocc/pdf/SROCC_FinalDraft_FullReport.pdf), 2019.

441 Notz, D.: Sea-ice extent and its trend provide limited metrics of model perfor
442 mance, *Cryosphere*, 8, 229–243, <https://doi.org/10.5194/tc-8-229-2014>, 2014.

443 O’Neill, B. C., Kriegler, E., Riahi, K., Ebi, K. R., Hallegatte, S., Carter, T. R.:
444 A new scenario framework for climate change research: the concept of s
445 hared socioeconomic pathways, *Climatic Change*, 122, 387–400. [https://doi.](https://doi.org/10.1007/s10584-013-0905-2)
446 [org/10.1007/s10584-013-0905-2](https://doi.org/10.1007/s10584-013-0905-2), 2014.

447 Richter-Menge, J., Druckenmiller, M. L., and Jeffries, M.: Arctic Report Card 2019,
448 <https://www.arctic.noaa.gov/Report-Card>, 2019.

449 Ryan, C., Thomas, G., and Stagonas, D.: Arctic Shipping Trends 2050, [https://](https://doi.org/10.13140/RG.2.2.34680.67840)
450 doi.org/10.13140/RG.2.2.34680.67840, 2020.Screen, J. A., and Simmonds,
451 I.: Increasing fall-winter energy loss from the Arctic Ocean and its role in
452 Arctic temperature amplification, *Geophys. Res. Lett.*, 37, [https://doi.org/10.](https://doi.org/10.1029/2010gl044136)
453 [1029/2010gl044136](https://doi.org/10.1029/2010gl044136), 2010.

454 Serova, N. A., and Serova, V. A.: Critical tendencies of the transport infrastruc
455 ture development in the Russian Arctic. *Arctic and North*, 36, 42–56, [http](http://doi.org/10.17238/issn2221-2698.2019.36.42)
456 [s://doi.org/10.17238/issn2221-2698.2019.36.42](http://doi.org/10.17238/issn2221-2698.2019.36.42), 2019.

457 Shu, Q., Wang, Q., Song, Z. Y., Qiao, F. L., Zhao, J. C., Chun, M.: Assessm
458 ent of sea ice extent in CMIP6 with comparison to observations and CMI
459 P5. *Geophys. Res. Lett.*, 47, e2020GL087965, <https://doi.org/10.1029/2020G>
460 L087965, 2020.

461 SIMIP Community: Arctic sea ice in CMIP6, *Geophys. Res. Lett.*, 47, e2019G
462 L086749, <https://doi.org/10.1029/2019GL086749>, 2020.

463 Smith, L. C., and Stephenson, S. R.: New Trans-Arctic shipping routes navigable by
464 midcentury, *P. Nati. Acad. Sci. USA*, 110, E1191–E1195,
465 <https://doi.org/10.1073/pnas.1214212110>, 2013.

466 Stephenson, S. R., Smith, L. C., Brigham, L. W., and Agnew, J. A.: Projected 21st-
467 century changes to Arctic marine access, *Climatic Change*, 118, 885–
468 899, <https://doi.org/10.1007/s10584-012-0685-0>, 2013.

469 Streng, W., Eger, K. M., Flistad, B., Jgensen-Dahl, A., Lothe, L., Mejlnder-Lar
470 sen, M., Wergeland, T.: Shipping in Arctic waters: a comparison of the n
471 ortheast, northwest and trans polar passages, <https://doi.org/10.1007/978-3-6>
472 42-16790-4, 2013.

473 Tillman, H., Yang, J., and Nielsson, E. T.: The Polar Silk Road: China's New
474 Frontier of International Cooperation. *China Quarterly of International Strat*
475 *egic Studies*, 04(03), 345–362, <https://doi.org/10.1142/S2377740018500215>,
476 2019.

477 Transport Canada: Arctic Ice Regime Shipping System (AIRSS) Standards (Ott
478 wa), Transport Canada, Ottawa, <https://tc.canada.ca/en/marine-transportation/a>
479 rcticshipping/arctic-ice-regime-shipping-system-airss, 1998.

480 Yu, M., Lu, P., Li, Z. Y., Li, Z. J., Wang, Q. K., Cao, X. W., Chen, X. D.:
481 Sea ice conditions and navigability through the Northeast Passage in the p
482 ast 40 years based on remote-sensing data. *Int. J. Digit. Earth*, 1–20, <https://doi.org/10.1080/17538947.2020.1860144>,
483 2020.